IOP PUBLISHING JOURNAL OF PHYSICS D: APPLIED PHYSICS

J. Phys. D: Appl. Phys. **43** (2010) 455411 (6pp) doi:10.1088/0022-3727/43/45/455411

Growth mechanism of cuboid growth pits in lead selenide epilayers grown by molecular beam epitaxy

J G Ma[1], M E Curtis[2], M A Zurbuchen[3], J C Keay[2], B B Weng[1], D H Li[1], F H Zhao[1], M B Johnson[2] and Z Shi[1]

[1] School of Electrical and Computer Engineering, University of Oklahoma, Norman, OK 73019, USA
[2] Department of Physics and Astronomy, University of Oklahoma, Norman, OK 73019, USA
[3] The Aerospace Corporation, 2350 E. El Segundo Blvd. M2-244El Segundo, CA 90245, USA

E-mail: jgma@ou.edu

Received 21 July 2010, in final form 18 September 2010
Published 27 October 2010
Online at stacks.iop.org/JPhysD/43/455411

Abstract

Microstructures and crystallographic orientations of cuboid growth pits in lead selenide (PbSe) epilayers grown on Si (1 1 1) by molecular beam epitaxy (MBE) have been studied by scanning electron microscopy and cross-sectional transmission electron microscopy. Cuboid density was found to be dependent on MBE growth parameters such as sample thickness and substrate temperature. Cuboid growth defects nucleate spontaneously on the PbSe growth surface probably at Pb droplets. This nucleation results in randomly oriented PbSe crystallites that preferentially grow along the [1 0 0] axis of the NaCl-type crystal structure. This preferential growth results in cuboid crystallites with cubic faces protruding from the epitaxial (1 1 1) face.

(Some figures in this article are in colour only in the electronic version)

1. Introduction

Due to their special physical and chemical properties, such as low Auger recombination coefficients, nearly equal electron and hole masses, and low thermal conductivities, lead-salt materials have been used in many solid-state devices including mid-infrared (IR) light-emitting and laser diodes [1, 2], mid-IR sensors [3] and thermoelectric coolers and generators [4]. Until the invention of the quantum cascade laser, lead-salt based laser diodes were the only available mid- and far-IR products on the market. Still, the easy and large tunability, and low threshold offer attraction for gas sensing applications. For IR sensor application, uncooled lead-salt photoconductive detectors have been widely used for various industrial purposes and have the potential for low-cost thermal imaging [5]. In fact, recently, monolithic photovoltaic PbTe-based focal plane arrays, sensitive in the 3–5 mm range, have been grown on Si substrates with integrated read-out electronics [6]. However, much less effort has been made in lead salt materials in comparison with their III–V and II–VI counterparts. Significant progress in IV–VI based IR devices can be expected if more efforts are made to improve the quality of IV–VI materials.

Recently, much effort has been devoted to improving material quality and understanding the formation of dislocations and other growth defects in IV–VI materials [7–9]. It was found that one prevalent type of growth defect in molecular beam epitaxy (MBE) grown PbSe epitaxial layers, the so-called 'cuboid growth pits', was composed of single or multiple micrometre-sized PbSe crystals with their geometric structures embedded in the PbSe (1 1 1) epilayers [9]. For the prevailing II–VI and III–V materials such as $Hg_{1-x}Cd_xTe$ and $In_{1-x}Ga_xAs$, the formation of various growth defects such as twins, craters, hillocks and V-shaped defects has been intensively studied and different models have been proposed to explain the growth mechanisms [10–12]. To the best of our knowledge, similar studies of IV–VI materials have not been done. In this paper, we present an extensive investigation of growth pits in PbSe epilayers grown by MBE on Si (1 1 1) substrates. The microstructure and growth mechanism of the cuboid growth pits are discussed.

2. Experimental procedures

PbSe epilayers were grown on Si (1 1 1) substrates using a very thin CaF_2 buffer layer in a custom-designed MBE apparatus. The PbSe growth was performed using a Se enriched PbSe binary source (1% mole excess) and an elemental Se source. A fixed Se-to-PbSe flux ratio of 0.1 and a growth rate of 2.0 μm per hour were used for all growths reported. Further details concerning the sample growth have been described elsewhere [7]. Scanning electron microscopy (SEM) and electron backscattered diffraction (EBSD) were performed in a Quanta 600 FESEM. Cross-sectional transmission electron microscopy (TEM) was carried out with a JEOL 2010F field-emission TEM. The TEM sample preparation was performed by focused ion beam (FIB) milling. Compositions of the epilayer and cubiod defects were confirmed by energy dispersive spectroscopy (EDS) to be composed exclusively of Pb and Se.

3. Results

Typical morphologies of PbSe (1 1 1) epilayers grown on Si (1 1 1) substrates are shown in figure 1. The differential interference contrast (DIC) optical micrograph, figure 1(*a*), clearly shows an 'orange peel' surface, indicating high-quality crystal growth. A few large cuboid growth pits of various shapes and a number of smaller defects, ranging from less than one-half to several micrometres in size are present. The plan-view SEM image, figure 1(*b*), shows that the large growth pits are composed of multiple-faceted features with cubic symmetry and have been named 'PbSe cuboids' [9]. These cuboids are typically found as single cubes, but also form larger conglomerates of multiple cubes. The small features visible in figures 1(*a*) and (*b*) are hemispherical in shape and are thought to be Pb droplets as described by Smith and Pickhardt [13]. The inset of figure 1(*b*) is a high-resolution oblique-view SEM image of two droplets on the PbSe surface. The cross-sectional SEM image, figure 1(*c*), shows a cluster of PbSe cuboids. The major part of the cuboid cluster is embedded in the PbSe epilayer with the root of its structure about 4 μm below the epitaxial surface and about 3 μm above the Si/CaF_2/PbSe interfaces. Also apparent in this image, and not unique to this cuboid, is the depletion of material surrounding the root of the structure. For simplicity, the rest of this work will focus on cuboid growth pits containing a single PbSe cuboid. The images of figure 1 strongly suggest the cuboids are {1 0 0} faces of a PbSe crystallite embedded in the (1 1 1) epitaxial PbSe epilayer. To confirm the orientations of the epilayer and cuboids, we performed EBSD on a single cube shaped defect.

A plan-view SEM image of a growth pit containing a typical cuboid is shown in figure 2(*a*). The top facet of the cuboid has a flat profile at a slight inclination to the (1 1 1) surface of the PbSe epilayer. Material depletion is apparent along the edges of the cubic structure, as are 'bridges' to the epilayer on the corners. For the EBSD measurements, the sample was tilted 70° from the electron beam and the accelerating voltage was 20 kV. Figures 2(*b*) and (*c*) are backscatter diffraction images overlaid with the computed crystallographic orientation of the epilayer and cuboid, respectively, at 70° from normal incidence. The insets of figure 2(*a*) are EBSD-calculated unit cells of the epilayer (lower left) and cuboid (lower right) with respect to the normal of the epilayer surface. From these results, we find the growth orientation of PbSe epilayer is along the [1 1 1] direction, consistent with the orientation of the Si(1 1 1) substrate. The exposed flat surface of the PbSe cuboid is a {1 0 0} PbSe plane several degrees off the normal of the epilayer surface. The less exposed side faces are also {1 0 0}

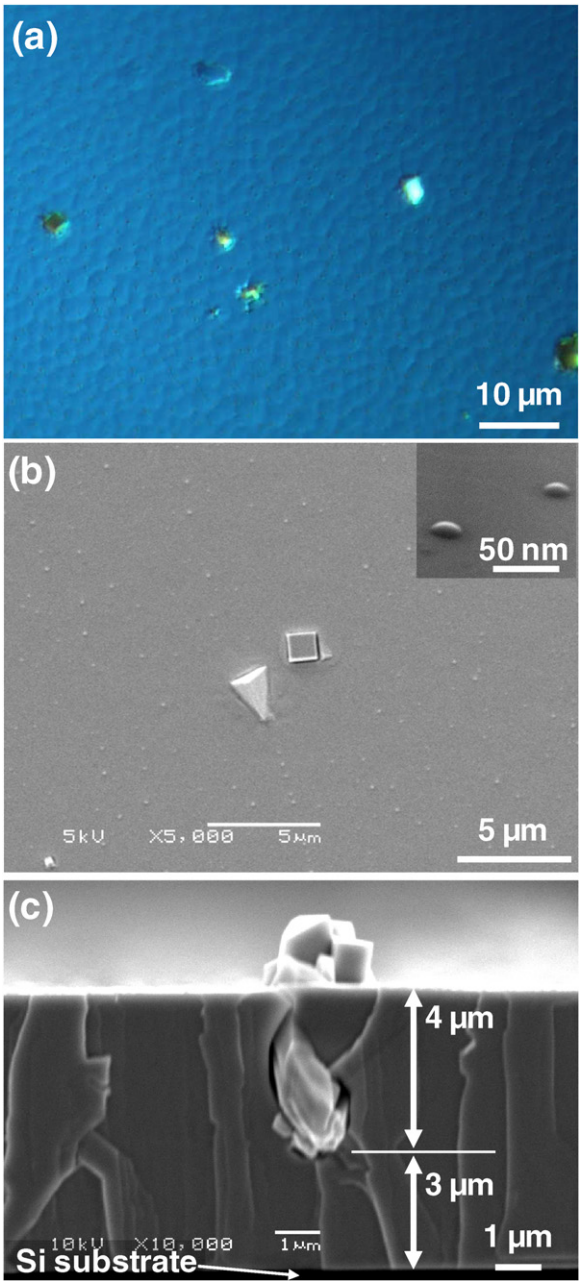

Figure 1. (*a*) DIC optical microscope image of cuboids in a PbSe (1 1 1) epilayer. (*b*) Plan-view SEM image of two cuboids in the PbSe (1 1 1) epilayer. The inset is a high-resolution oblique-view SEM image of two droplets on the PbSe surface. (*c*) Cross-sectional SEM image of cleaved face showing a cluster of PbSe cuboids including the root structure in the PbSe (1 1 1) epilayer. The Si(1 1 1) substrate is the dark uniform layer at the bottom, as labelled.

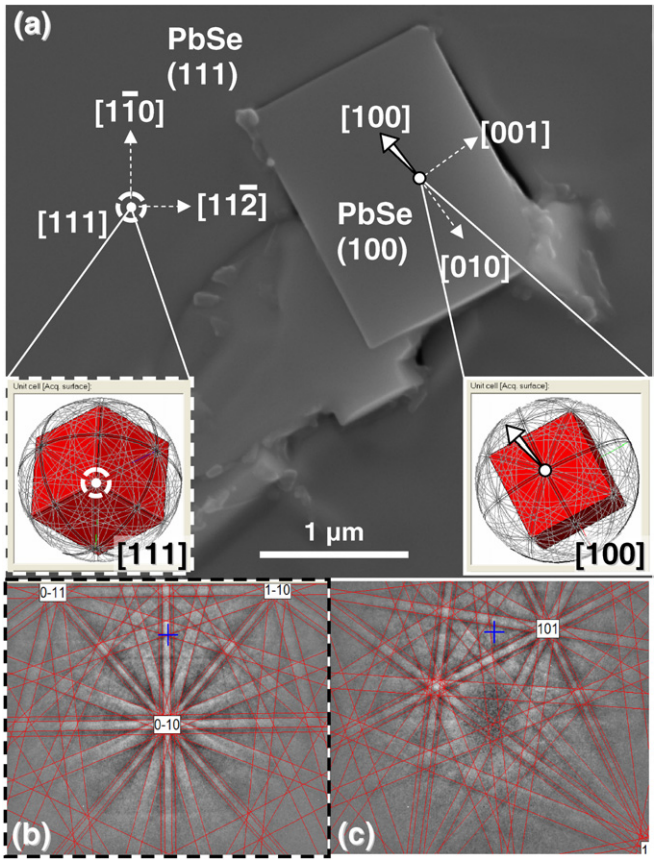

Figure 2. (*a*) Top down SEM image of a PbSe cuboid with the orientation of the cuboid and epilayer labeled. Electron backscattered diffraction images from the epilayer (*b*) and cuboid (*c*) at 70° from normal, overlaid with calculated indices. Insets in (*a*) are the EBSD-calculated unit cells oriented relative to the direction of the surface normal, for the epilayer (bottom left, dashed) and cuboid (bottom right, solid), respectively.

planes. Therefore, the exposed faces of the PbSe cuboid are {1 0 0} planes of the NaCl-type structure, indicating the cuboid grows in a different mode compared with the surrounding PbSe epilayer.

In order to better elucidate the initial growth of the PbSe cuboids, we performed cross-sectional TEM on a cuboid similar to the one shown in figure 2(*a*). The cuboid was sliced along the [1 0 0] direction at its centre by FIB milling to obtain a sample for cross-sectional observation. Prior to the FIB milling, a platinum thin film was sputter deposited on the sample surface to secure the cuboid to the epilayer during the FIB processing and post-process handling. Figure 3 shows a set of TEM micrographs of the cross-sectioned cuboid. Figure 3(*a*) shows a montage of cross-sectional bright field (BF) TEM images of the complete cuboid, which allow one to trace back to the initial stage of the PbSe cuboid growth (arrow indicates the [1 1 1] orientation of the Si substrate as well as the film growth direction). The head of the cuboid is about 300 nm higher than the surface of the epilayer, and is separated from the surrounding epilayer by ∼100 nm gaps. The cuboid has a spindle like shape with a nearly rectangular head tapering towards its root. A dark field (DF) TEM image of the same cuboid is shown in figure 3(*b*) with $g = (0\,1\,0)$. The variation of image contrast in the lower part of the cuboid in figure 3(*b*) indicates bending, likely due to strain in the cuboid during its initial growth. The contrast is more uniform in the upper part of the cuboid where the shape becomes more rectangular. Figure 3(*c*) shows a higher magnification BF TEM image of the root of the cuboid which locates it in the middle of the epilayer. This again indicates that the formation of the cuboid does not initiate at the interface between the Si and PbSe, but spontaneously during the epitaxial growth. Selected area electron diffraction (SAED) patterns and high resolution TEM (HRTEM) image of the PbSe cuboid are shown in figures 3(*d*) and (*e*), respectively. Complementary, SAED patterns and HRTEM images of the PbSe epilayer are shown in figures 3(*f*) and (*g*), respectively. A single set of ED patterns and clear lattice fringes indicate the single-crystal nature of the PbSe epilayer and the the PbSe cuboid. In addition, the ED patterns of the cuboid show that the top edge of the cuboid is nearly parallel to the [1 0 0] direction, consistent with the EBSD results. We were not able to directly observe any remnant of the droplet at the root of the cuboid in our cross-sectionally prepared samples.

In order to investigate the effects of MBE growth conditions on the cuboid growth pit density, a series of epitaxial growths were performed with variations of the substrate temperature and sample thickness. The cuboid densities were obtained by areal counting in DIC microscope images. Figure 4(*a*) shows the dependence of cuboid density on substrate temperatures for a fixed epilayer thickness of 4.5 μm. It can be seen in figure 4(*a*) that the effect of the substrate temperature on the cuboid density is not monotonic. The density is about 4000 cm^{-2} at 370 °C, and reaches its maximum (∼13 000 cm^{-2}) at a substrate temperature of 400 °C. Further increasing the substrate temperature to 425 °C, the density decreases to 7000 cm^{-2}. Figure 4(*b*) shows the relationship between the cuboid density and the thickness of epilayer. From this data, one can see that the density increases monotonically with increasing sample thickness for the substrate temperatures of 370 and 400 °C and that the cuboids appear to nucleate only after the PbSe films have been grown for some time.

4. Discussion

In this section, we interpret the data to show that the cuboid defects form spontaneously during MBE growth according to the following sequence. The cuboids are thought to nucleate at Pb droplets that occur on the growth surface. The Pb droplets nucleate randomly oriented PbSe crystallites that preferentially grow with exposed {1 0 0} surfaces forming embedded cuboids in the PbSe (1 1 1) surface. The cuboids protrude from the (1 1 1) surface, and exposed {1 0 0} planes giving their cubic shape. We start by discussing the formation of Pb droplets on the PbSe growth surface and how this results in the non-monotonic cuboid density versus temperature behaviour. We conclude with a discussion of cuboid growth after nucleation.

It is useful to begin by noting the nature of MBE growth of IV–VI materials. Generally, for MBE growth of IV–VI materials, binary compound sources like PbTe and PbSe are employed because IV–VI compounds sublime

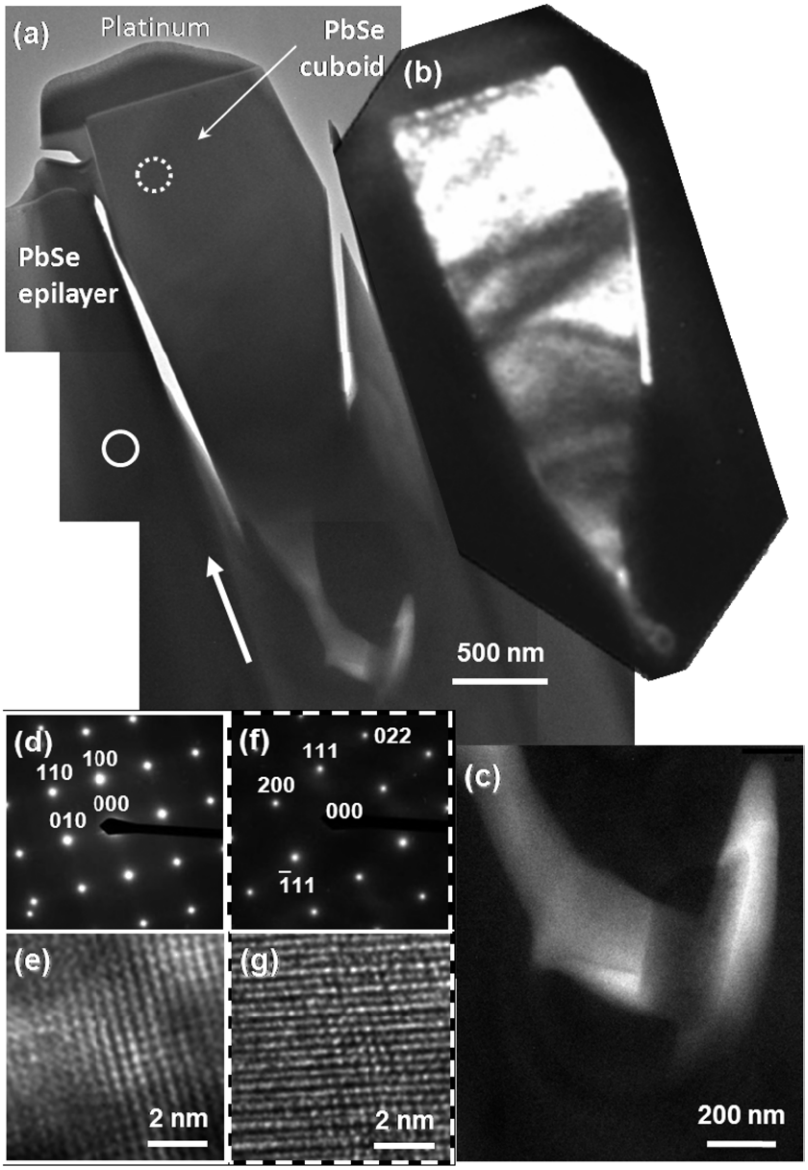

Figure 3. (*a*) Bright field TEM image of the top of the PbSe cuboid. (*b*) Dark field TEM image of the same cuboid with $g = (0\,1\,0)$. (*c*) Higher magnification bright field TEM of the root of the cuboid. (*d*) and (*e*) PbSe cuboid SAED pattern and HRTEM image, respectively. (*f*) and (*g*) PbSe epilayer SAED pattern and HRTEM image, respectively.

congruently [14]. It has been found that for typical MBE effusion cell temperatures of 600–700 °C, the molecular content of the vapour phase in equilibrium with bulk PbSe is about 95% and about 97% for PbTe [15]. Growths, however, are typically carried out under non-equilibrium conditions and the fraction of dissociated and secondary group IV and VI vapour species such as Pb and Se_2 cannot be neglected. At the normal substrate temperatures for MBE growth, the re-evaporation rate of Se is many orders of magnitude higher than that of the PbSe compound, implying that no secondary Se phase will be formed on the substrate surface. However, the situation is completely different for the dissociated Pb adatoms, because their re-evaporation rate is of the same order of magnitude as PbSe, Thus, most Pb adatoms will remain on the surface under normal MBE growth conditions. It is known that the (1 1 1) surface of the PbSe epilayer will be Pb stabilized except under deliberately high Se partial vapour pressure [16]. Smith and Parkhardt have found that at a substrate temperature of 380 °C ($Pb_{(1-x)}Sn_xTe$), only 0.1% of the impinging excess Pb atoms were incorporated into the film during MBE growth, and the remainder of excess Pb atoms diffused on the surface and coalesced into micrometre-sized droplets in order to minimize the surface energy [13]. As indicated in figures 1(*a*) and (*b*), we also see evidence of such Pb droplets, though they are much smaller (20–200 nm in diameter). Although the provision of supplemental Se via a Se rich PbSe binary effusion source and a separate Se effusion source supplies ∼10% excess Se in the beam flux, excess Pb is not completely eliminated, probably due to the high re-evaporation rate of Se. In fact, in related work where the flux from the Se source was substantially increased, no change in the defect density was observed.

The continual coalescence of Pb on the PbSe surface and the linear increment of the cuboid density suggest that the PbSe

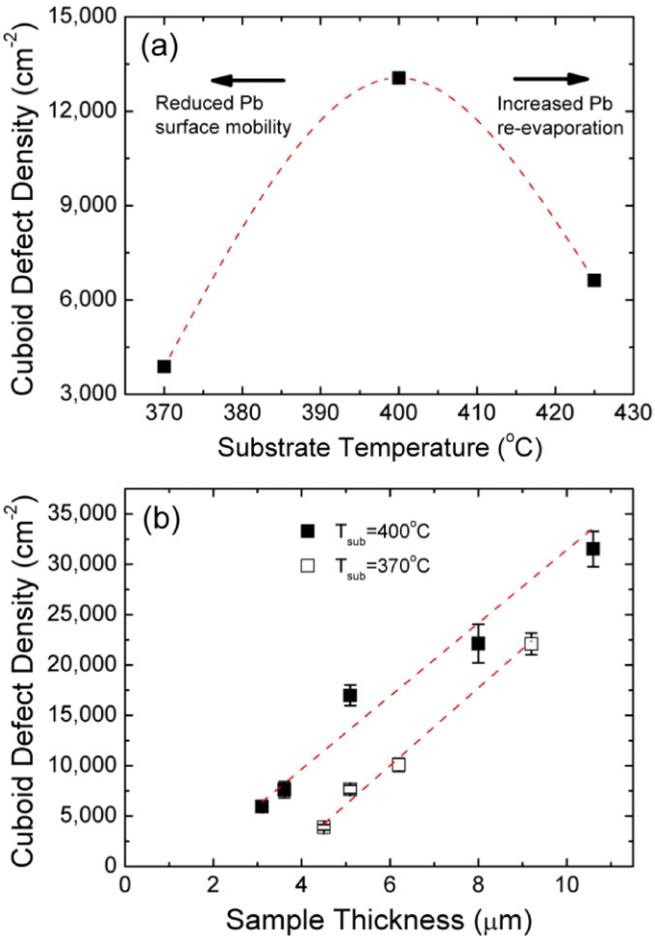

Figure 4. (*a*) Cuboid densities versus substrate temperatures for a given sample thickness of 4.5 μm. (*b*) Cuboid densities versus sample thicknesses for substrate temperatures of 370 °C (hollow squares) and 400 °C (solid squares). The dotted lines are guides to the eye.

cuboids initiate growth on, or within, the Pb droplets. Within this liquid environment, the cuboids can easily acquire their observed characteristics: high-quality (1 0 0) growth, random orientation of cube faces and spontaneous initiation at any time during epilayer growth. Thus the density of Pb droplets will determine the cuboid density. The size and density of Pb droplets on the growth surface are a delicate balance of diffusion of Pb to the droplet and re-evaporation of lead from the growth surface and the droplets. Both diffusion and re-evaporation involve activated processes. The diffusion rate involves the diffusion coefficient, D_s, which is proportional to $\exp(-E_s/k_BT)$, where E_s is an activation energy, k_B is the Boltzmann constant and T is the temperature in K. The re-evaporation rate of Pb adatoms is given by [17]

$$I_{\mathrm{re-evap}}(\mathrm{atom\,cm^{-2}\,s^{-1}}) = a_v \cdot \frac{\exp(B - (A/T(\mathrm{K})))}{\sqrt{M(\mathrm{g\,mol^{-1}}) \cdot T(\mathrm{K})}}, \qquad (1)$$

where α_v is the evaporation coefficient, $B = 21\,161$ and $A = 18.027$ are the material-related constants which are extracted from [17, 18] and M is the molar weight. According to equation (1), the re-evaporation rate of Pb adatoms at 425 °C is one order of magnitude higher than that at 375 °C. The Pb diffusion and re-evaporation rate are in opposition for the formation of a Pb droplet capable of nucleating a cuboid. Therefore, a reasonable argument for the behaviour of cuboid density with temperature is that at lowest temperature investigated, diffusion limits the supply of Pb to the droplets and at the highest temperature re-evaporation limits the Pb droplet size and density. As the temperature increases from the minimum growth temperature, there is an increased diffusive Pb supply to the droplets and the cuboid density increases, and at higher temperatures, the effects of re-evaporation dominate and the cuboid density decreases. While other processes may influence cuboid nucleation and growth, this model serves as a framework for analysis. Once formed, the growth of {1 0 0} faces is expected, based on the lower free-energy of these surface versus {1 1 1} surfaces. The observation that the cuboids protrude out of the (1 1 1) surface (often by up to 1 μm) supports this. This difference in growth rate cannot be associated with differences in the flux of constituents impinging on the surfaces. Therefore, the difference in growth rate must be associated with either a difference in the re-evaporation from the two surfaces or diffusion of material to the {1 0 0} cuboid faces from the surrounding (1 1 1) epitaxial surface. The former is unlikely to be sufficient at lower growth temperatures because, even though {1 0 0} surfaces have a lower free-energy than {1 1 1} surfaces and thus a lower re-evaporation rate, the Pb re-evaporation rate at 380 °C for the (1 1 1) surface is only about 4% of the growth rate [17] and PbSe re-evaporation is even less. Considering the extreme example of a 4% loss for the (1 1 1) surface and 0% loss for the (1 0 0) surface, it is clear that this is insufficient to explain the growth rate discrepancy. Thus, it is more likely that Pb and PbSe diffuse from the (1 1 1) epitaxial surface to the {1 0 0} faces. Initially this seems unlikely given the very deep, narrow trenches that separate the cuboids from the surrounding epitaxial surface. However, plan-view SEM images indicate that for all cuboids observed, smooth bridges that connect cuboid to epilayer are seen on at least one side or edge. As well, our direct measurements of the Pb diffusion length for the (1 1 1) surface is several micrometres at typical growth temperatures[4], which is sufficient to explain the growth rate discrepancy. Widely spaced Pb droplets (~1 per [100 μm]^2) can form new PbSe cuboids without overlap. Thus, it is reasonable to say that the formation of Pb droplets at any stage of MBE growths is constant, yielding the observed monotonic increase in cuboid density with the PbSe film thickness.

The fact that no droplet remnant was observed in the cross-section TEM work is not surprising. This is partially because the cross-sectionally prepared samples are 80–100 nm thick and would have about a 10% chance of even capturing the nucleation point of a > 1 μm sized cuboid. Furthermore, finding a nanometre-sized remnant in a thin slice is difficult, especially if all that remains is a Pb-rich region of PbSe.

[4] Atomic force microscope images show no Pb droplets within about 5 μm of widely spaced, atomic-sized steps on PbSe layers grown on cleaved BaF_2 (1 1 1) substrates (unpublished).

5. Conclusion

In summary, the microstructure and formation of growth pits in PbSe epilayers grown on Si (1 1 1) substrates by MBE were studied by SEM and TEM. Both EBSD and SAED indicated that the exposed cuboid faces are {1 0 0} PbSe planes. Cross-sectional TEM confirmed the mono-crystalline nature of PbSe cuboids and revealed the evolution of PbSe cuboids. Based on the dependence of cuboid density on substrate temperatures and sample thicknesses, the nucleation of PbSe cuboids in growth pits is assigned to Pb droplets on the epitaxial growth front.

Acknowledgments

Funding for this work was provided by the STTR program of the Missile Defense Agency under Contract No HQ0006-07-C-7657, the US DoD ARO under Grant W911NF-07-1-0587, DEPSCoR W911NF-04-1-0259, the Aerospace Independent Research and Development Program, and by NSF DMR-0520550.

References

[1] Partin D L 1988 *IEEE J. Quantum Electron.* **24** 1716
[2] Tacke M 1995 *Infrared Phys. Technol.* **36** 447
[3] Zogg H 1999 *Proc. SPIE* **3890** 22
[4] Harman T C, Taylor P J, Walsh M P and LaForge B E 2002 *Science* **297** 2229
[5] Vergara G, Gutiérrez R and Gómez L J 2009 *Proc. SPIE.* **7298** 729829
[6] Zogg H, Alchalabi K, Zimin D and Kellermann K 2003 *IEEE Trans. Electron Devices* **50** 209
[7] Zhao F, Mukherjee S, Ma J, Li D, Elizondo S L and Shi Z 2008 *Appl. Phys. Lett.* **92** 211110
[8] Wiesauer K and Springholz G 2004 *Phys. Rev.* B **69** 245313
[9] Ma J G, Li D H, Bi G, Zhao F H, Elizondo S, Mukherjee S, Shi Z 2009 *J. Electron. Mater.* **38** 325
[10] Aoki T, Chang Y, Badano G, Zhao J, Grein C, Sivananthan S and Smith D J 2004 *J. Cryst. Growth* **265** 224
[11] Zandian M, Arias J M, Bajaj J, Pasko J G, Bubulac L O and Dewames R E 1995 *J. Electron. Mater.* **24** 1207
[12] Lytvyn P M, Prokopenko I V, Strelchuk V V, Mazur Yu I, Wang Zh M and Salamo G J 2005 *J. Cryst. Growth* **284** 47
[13] Smith D L and Pickhardt V Y 1976 *J. Electron. Mater.* **5** 247
[14] Lin J C, Sharma R C and Chang Y A 1996 *J. Phase Equilib.* **17** 253
[15] Novoselova A V and Zlomanov V P 1981 *Current Topics in Materials Science* 7th edn, ed E Kaldis (Amsterdam: North-Holland) p 643
[16] Springholz G and Bauer G 1995 *J. Appl. Phys.* **77** 540
[17] Springholz G 2003 *Lead Chalcogenides: Physics and Applications* ed D Khokhlov (New York: Taylor and Francis) p 132
[18] Glang R 1970 *Handbook of Thin film Technology* ed L I Maissel and R Glang (New York: McGraw-Hill) pp 1–3